Kinetics and Molecular Modelling Studies on the Stereoselective Hydrolysis of Enantiomeric Esters by Dipeptide Catalysts

Yasuji Ihara,*[a] Satoko Asakawa,[a] Kayo Igata,[a] Yōko Matsumoto[b] and Ryuichi Ueoka[b]
[a] *Yamaguchi Women's University, 3-2-1 Sakurabatake, Yamaguchi 753, Japan*
[b] *Department of Industrial Chemistry, Kumamoto Institute of Technology, Ikeda, Kumamoto 860, Japan*

The rate constants of the catalytic hydrolysis of short and long chain *N*-acylphenylalanine *p*-nitrophenyl esters by a series of optically active dipeptide catalysts in the presence of surfactant aggregates are presented in order to evaluate their catalytic efficiency and stereoselectivity. Circular dichroism spectra of dipeptide catalysts have also been measured in order to estimate the most probable and stable conformation in micellar solution. On the basis of the kinetic stereoselectivities and CD spectra, molecular modelling studies have been performed in order to determine the preferred conformations and energies of dipeptide catalysts and chiral substrates in the presence of surfactants. An analysis of minimum-energy conformations obtained from the calculation reproduces the sense of the kinetic stereoselectivities.

The stereospecificity is one of the most interesting properties in enzymatic reactions.[1] The stereoselective hydrolysis of enantiomeric esters has been recently attracting considerable attention in connection with understanding the origins of the stereoselectivity observed with proteolytic enzymes.[2–8] We have previously described a series of studies on stereoselective micellar catalysis in the hydrolysis of enantiomeric esters by optically active catalysts containing a histidyl group.[9–16]

We found[14a,b] that both the rate constants and the stereoselectivity for the reaction of substrates **3c**, **d** with the dipeptide catalysts **2a–f** (which have L,L configurations) increase to a maximum and then decrease as the amino acid side groups of the catalysts become larger and more hydrophobic. Thus the largest stereoselectivities were attained by using the catalysts of Z-Leu-His (**2c**) and Z-Phe-His (**2e**).

In order to gain further insight into the stereoselective micellar catalysis and to understand the relationship between molecular structures and the stereoselectivity, we examined catalytic cleavages of short and long chain *N*-acylphenylalanine *p*-nitrophenyl esters by a series of dipeptide catalysts in the presence of surfactant aggregates. Circular dichroism spectra of dipeptide catalysts were also measured in order to estimate the most probable and stable conformation in micellar solution. Finally, we attempted to predict the conformation of one of the dipeptide catalysts employed in this study on the basis of computer modelling studies. An empirical conformation energy was calculated by assuming that the catalyst in the presence of surfactant micelles is analogous to the general polypeptide structures. The relationship between stereoselectivity and the conformation of dipeptide catalysts is discussed.

Experimental

Materials.—All materials used in this experiment have been described elsewhere.[11–14]

Kinetic Measurements.—Reactions were generally monitored on a Hitachi 200 spectrophotometer or a Shimadzu 140 spectrophotometer with a thermostatted cell holder at 25 °C. In the general procedure, a solution (25 mm^3) of ester in acetonitrile was added to a buffer solution (3.00 cm^3) containing the catalyst and surfactant at desired concentrations. The hydrolysis of the substrates was examined under pseudo-first-order conditions, [surfactant] > [catalyst] > [substrate], at pH 7.30, 0.02 mol dm^{-3} Tris-HCl buffer. The rate constant k_{obs} was determined by monitoring the release of the *p*-nitrophenolate ion at 400 nm. Kinetics were first order and good least-squares rate constants were obtained ($r > 0.999$) over at least two half-lives. From three or more reactions, we estimate that rate constants are reproducible within ±5%.

Circular Dichroism.—The CD spectra of peptide catalysts were measured on a Jasco J-50A recording spectropolarimeter (Xe lamp, 1.0 cm cell) in the presence of CTAC micelles at room temperature. The concentration of peptide catalysts was 2.5×10^{-4} mol dm^{-3}.

Calculation Method.—The calculations were mostly performed on an NEC personal computer with the ECEPP program[17] combined with a program which can present a minimum of a several torsional variables and with a NAMOD[18] graphics terminal. The values of all bond lengths and bond angles were fixed in the calculations. Charges on the atoms of catalysts and substrates were estimated from MNDO[19] calculations in respect of *N*-methoxycarbonyl-L-phenylalanyl-L-histidine methyl ester and *N*-acetyl-L-phenylalanine methyl ester, with full geometry optimization.

Results and Discussion

Kinetic Studies.—Kinetic studies were examined at 25 °C using pH 7.30 Tris-HCl buffer in 0.83% (v/v) acetonitrile–water at a fixed [CTAB] of 2.00×10^{-3} mol dm^{-3}. Under the conditions [catalyst] ≫ [substrate], pseudo-first-order rate constants (k_{obs}) were evaluated by monitoring the release of *p*-nitrophenoxide ion spectrophotometrically at 400 nm. The apparent second-order rate constant (k_c) was evaluated by the following eqn. (1), where $k_{surfactant}$ refers to the observed first-order rate constant without a catalyst in the presence of surfactant micelles.

$$k_c = (k_{obs} - k_{surfactant})/[\text{catalyst}] \quad (1)$$

The results of catalytic hydrolysis of substrates **3a**, **b** with various dipeptide catalysts having L,L configurations in the presence of CTAB micelles are summarized in Table 1, together with previous results for substrate **3c**. As expected, some of these catalysts for the hydrolysis of **3a**, **b** showed much larger stereoselectivities than in the case of **3c** under similar conditions. In the present catalytic systems, it is apparent that the catalysts

1, Z – His

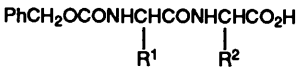

2

a; R^1 = Me, R^2 = CH_2Im (Z – Ala – His)
b; R^1 = Me_2CH, R^2 = CH_2Im (Z – Val – His)
c; R^1 = Me_2CHCH_2, R^2 = CH_2Im (Z – Leu – His)
d; R^1 = CH_2Im, R^2 = Me_2CHCH_2 (Z – His – Leu)
e; R^1 = $PhCH_2$, R^2 = CH_2Im (Z – Phe – His)
f; R^1 = 3 – indolyl – CH_2, R^2 = CH_2Im (Z – Trp – His)
Im = 4 – Imidazolyl

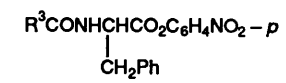

3

a; R^3 = Me, (Ac – Phe – ONp)
b; R^3 = $Me[CH_2]_{10}$ (Dod – Phe – ONp)
c; R^3 = MeO (Moc – Phe – ONp)
d; R^3 = $PhCH_2O$ (Z – Phe – ONp)

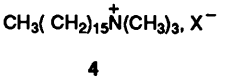

4

a; X = Br (CTAB)
b; X = Cl (CTAC)

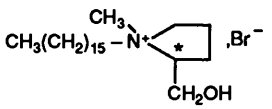

5, HPRB

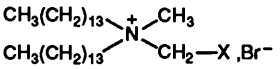

6

a; X = H (2C14)

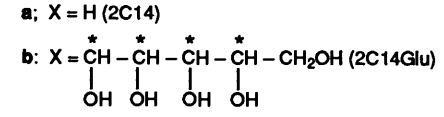

b: X = CH(OH) – CH(OH) – CH(OH) – CH(OH) – CH_2OH (2C14Glu)

Table 1 Rate constants and stereoselectivities (L/D) for the cleavage of enantiomeric substrates by dipeptide catalysts in the presence of CTAB[a]

	k_c/dm^3 mol^{-1} s^{-1}								
	Ac-Phe-ONp (**3a**)			Dod-Phe-ONp (**3b**)			Moc-Phe-ONp (**3c**)		
Catalysts	L	D	L/D	L	D	L/D	L	D	L/D
Z-L-His (**1**)				30	15	2.0	80.7	66.0	1.21
Z-L-Ala-L-His (**2a**)	64.8	17.0	3.8	72	20	3.6	139	32.1	4.3
Z-L-Val-L-His (**2b**)	239	23.8	10	225	26	8.7	309	44.7	6.9
Z-L-Leu-L-His (**2c**)	511	46.8	11	616	50	12	645	52.7	12
Z-L-His-L-Leu (**2d**)				12	5.5	2.2	54.5	47.0	1.2
Z-L-Phe-L-His (**2e**)	622	34.2	18	617	62	10	541	74.5	7.3
Z-L-Trp-L-His (**2f**)	113	33.8	3.3	76	51	1.5	85.9	47.2	1.8

[a] At pH 7.30, 0.02 mol dm^{-3}-Tris-HCl buffer, 25 °C, [CTAB] = 2.00 × 10^{-3} mol dm^{-3}, [Catalyst] = 1.00 × 10^{-4} mol dm^{-3}, [Substrate] = 1.0 × 10^{-5} mol dm^{-3}. From three or more reactions, we estimate that rate constants are reproducible within ±5%. [b] At pH 7.6, [CTAB] = 3.00 × 10^{-3} mol dm^{-3}.

containing a L-histidinyl residue preferentially hydrolyse the L-enantiomers of the substrates. The stereoselectivities for the dipeptide catalysts were greater than that for Z-L-histidine. The larger stereoselectivities observed with dipeptide catalysts suggest that the chirality of the amino acid residue adjusting to the histidine could play an important role in enhancing the stereoselectivity. The catalyst might have the appropriate orientation of the functional group and the stereochemical fit with a substrate.

In addition, the stereoselectivities of reactions with the dipeptide catalysts **2a**, **b**, **c**, **e** and **f** increase to a maximum and then decrease as the amino acid side groups of the catalysts becomes larger and more hydrophobic. This implies the importance of the combination of specific interactions such as steric, hydrophobic and hydrogen bonding in the course of the reaction. The structural effects in relation to stereoselectivities for these catalytic systems have been widely discussed in the previous papers.[10f,14,16c]

For the reaction in the micellar catalytic systems, the esters are incorporated onto their micellar phase and react with the imidazole group of a histidinyl residue in the catalysts. Therefore, it is now clear that the differences in stereoselectivity are attributable to the framework of the catalysts and are associated with the incorporation of the catalyst onto the surface of the surfactant domains leading to an effective interaction between catalyst and substrate. Thus the effective catalyst must have a suitable orientation of the imidazolyl group in catalysts and a stereochemical fit with a substrate. This suggests the importance of an appropriate combination of the sequence of amino acids including a histidyl unit and the hydrophobicity of the side chain in dipeptide catalysts in enhancing the stereoselectivity in the surfactant domains.

Recently, Ueoka *et al.*[16,20] demonstrated high stereoselective deacylation behaviour in the catalytic hydrolysis of long-chain enantiomeric esters by di- or tri-peptide catalysts in the presence of vesicular and co-aggregate surfactant systems. Moreover, Ohkubo *et al.*[21] found high stereoselectivity of short-chain esters in the catalytic vesicular system and at a low ionic strength. These results strongly suggest that the stereoselective hydrolysis in surfactant aggregates is easily controlled by changing the reaction field such as the composition of the aggregates, ionic strength, amino acid sequence in peptide catalysts, and the reaction temperature.

Table 2 summarizes the catalytic rate constants and stereoselectivities (L/D) for cleavage of two enantiomeric substrates **3a** and **b** by Z-Phe-His (**2e**) in the presence of several surfactant

Table 2 Rate constants for cleavage of enantiomeric esters **3a,b** by **2e** in the presence of surfactant aggregates[a]

	k_c/dm^3 mol^{-1} s^{-1}					
	Ac-Phe-ONp (**3a**)			Dod-Phe-ONp (**3b**)		
Surfactant	L	D	L/D	L	D	L/D
CTAB (**4a**)	622	34.2	18	617	62	10
HPRB (**5**)	458	34.9	13	471	66	7.1
2Cl4 (**6a**)	1160	65.7	18	1540	91	17
2Cl4Glu (**6b**)	487	3.8	130	612	74	8.3

[a] At pH 7.30, 0.02 mol dm^{-3}, Tris-HCl buffer and 25 °C. [CTAB or HPRB] = 2.00 × 10^{-3} mol dm^{-3}, [2Cl4 or 2Cl4Glu] = 1.00 × 10^{-3} mol dm^{-3}, [**2e**] = 1.00 × 10^{-4} mol dm^{-3}, [Substrate] = 1.0 × 10^{-5} mol dm^{-3}. From three or more reactions, we estimated that rate constants are reproducible to ±5%.

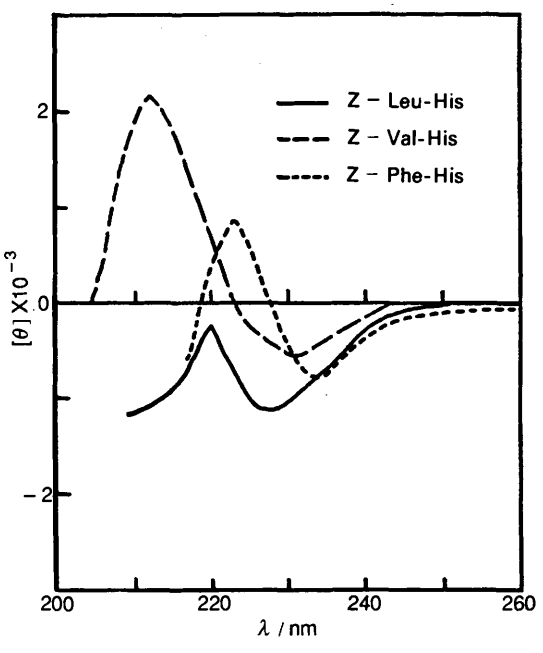

Fig. 1 CD Spectra of peptide catalysts with CTAC micelles in 5% (v/v) CH_3OH–H_2O; [Cat] = 2.5 × 10^{-4} mol dm^{-3} [CTAC] = 3.0 × 10^{-3} mol dm^{-3}

aggregates. It is found that the rate and stereoselectivity for the hydrolysis of both enantiomeric substrates show a remarkable dependency on the surfactant catalytic systems. Thus, reaction of short chain substrate **3a** with **2e** in vesicular **6b** gives the largest stereoselectivity. This shows that to achieve high stereoselectivity it is important for the chiral groups to be positioned near the polar head region of the surfactant, where the catalyst is very stable and capable of conforming to optimally fit one of the enantiomers. Thus, the orientation of the catalyst **2e** is rather more favourable on the short chain substrate **3a** than on the long-chain substrate **3b** in the surface of the glucose-substituted surfactant **6b**.[14d]

The above results strongly suggest that the selection of the kind of morphology of the surfactant aggregates, *i.e.*, the reaction field where the catalyst and substrate are incorporated into the surface of these coaggregates leading to an effective orientation between the reactants, is very important for the achievement of high stereoselectivity.

Circular Dichroism Spectra.—The CD spectra of dipeptide catalysts employed in this study were measured in the presence of CTAC micelles, as shown in Figs. 1 and 2. Interestingly, the specific CD spectra at *ca.* 227–235 nm occurred in Z-Leu-His, Z-Val-His and Z-Phe-His with CTAC micelles, which promoted

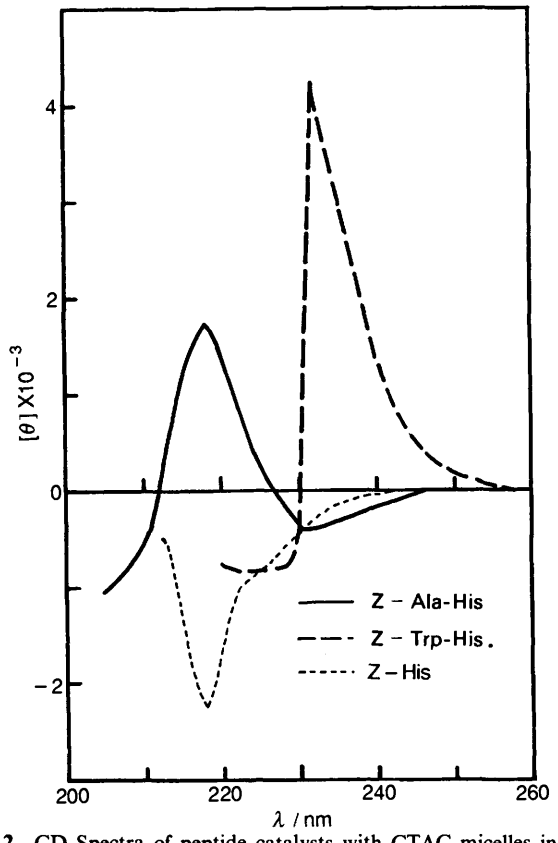

Fig. 2 CD Spectra of peptide catalysts with CTAC micelles in 5% (v/v) CH_3OH–H_2O; [Cat] = 2.5 × 10^{-4} mol dm^{-3} [CTAC] = 3.0 × 10^{-3} mol dm^{-3}

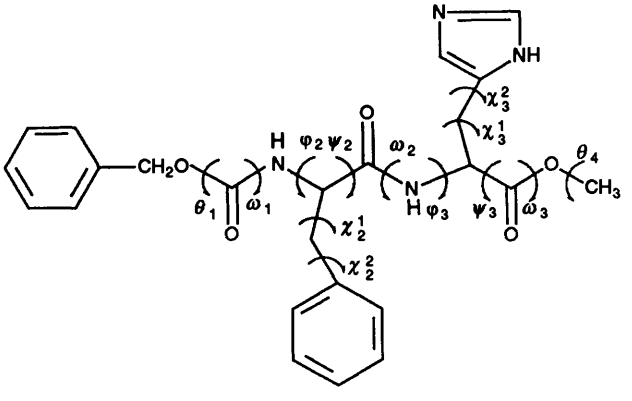

Fig. 3 Structural diagram of Z-Phe-His-OMe (7), with torsional angle labels

the relatively high enantioselectivity for the hydrolysis of the substrates. On the other hand, no specific CD spectrum at 235 nm was obtained in any of the inactive peptides (Z-His, Z-His-Leu, Z-Trp-His). The above data imply that these specific CD spectra at *ca.* 227–235 nm in active dipeptide catalysts bound to micelles of CTAC may support the α-helix [16c,22,23] or β-sheeted rigid conformation through the intra- or intermolecular interaction between amino acid residues.

On the basis of the above results, we are now attempting a more precise description of stereoselective catalyst conformers, using computer modelling along with hand-held models.

Conformational Energy Calculation.—Conformational energy calculation was performed on *N*-Benzyloxycarbonyl-L-phenylalanyl-L-histidine methyl ester (Z-Phe-His-OMe, **7**). The structural and energy parameters were taken from the ECEPP system. As shown in Fig. 3, we consider thirteen torsional angles

Table 3 Approximate torsional angles/° for some regular structures

		φ_2	ψ_2	φ_3	ψ_3
Right-handed helix		−57	−47	−57	−47
Chain pleated sheet	Parallel	−119	+113	−119	+113
	Antiparallel	−139	+135	−139	+135
Turn type structure	Type I	−60	−30	−90	0
	Type I′	+60	+30	+90	0
	Type II	−60	+120	+80	0
	Type II′	+60	−120	−80	0
	Type V	−80	+80	+80	−80

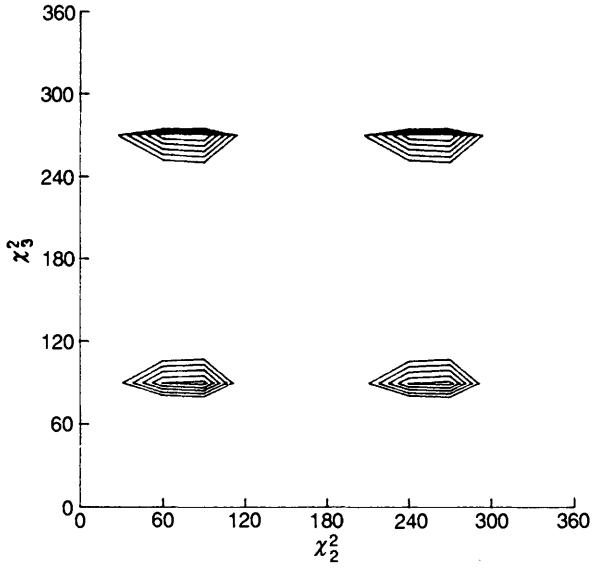

Fig. 4 Energy contour maps illustrating the variations of the side chain orientation of Phe (χ_2^2) and His (χ_3^2). Minimum point $\chi_2^2 = \chi_3^2 = 270$; $v_{min} = 0$ kcal mol^{-1}; interval = 1 kcal mol^{-1}; no. of lines = 5.

that determine the conformation of Z-Phe-His-OMe. For calculation, the main chain conformations were fixed to one of the standard conformations which are commonly obtained in the characteristic secondary structures of polypeptides[24] such as α-helix, β-sheet and turns as shown in Table 3. The amide bond was fixed in a planar *trans* (ω = 180°) conformation, and $\theta_1 = 180°$ and $\theta_4 = 180°$ were taken. For each main chain conformation, χ_2^1 and χ_3^1 in side chain rotational angles of Phe and His units were increased systematically by 60°, 180° and 300°, and χ_2^2 and χ_3^2 were varied from 0–360° at an interval of 30°. Initial energy calculations were performed in relation to *ca.* 12 000 starting conformations as defined above. One of the energy contour maps for the side-chain orientation of Phe and His units in the α-helix structure is shown in Fig. 4. Starting from the local minima in the side-chain energy maps, total energy minimization was then performed with respect to all torsional angles except for ω_1, ω_2 and ω_3. Some of the lowest energies among the local minima are listed in Table 4. The conformation of the lowest energy is obtained from one of the β-sheet starting structure and the energy was estimated to be −3.6 kcal mol^{-1}. No minimum lower in energy than the three conformers starting from the above structures could be found. The energy calculation study was also carried out on *N*-acetyl-L-phenylalanine methyl ester (Ac-Phe-OMe). For computational simplicity we calculated the structure of the methyl ester of acetyl phenylalanine, instead of the *p*-nitrophenyl ester **3a** which was actually used in our experiments. In Fig. 5 are shown NAMOD molecular display drawings for the four possible conformations of the catalyst. The minimum structures of these

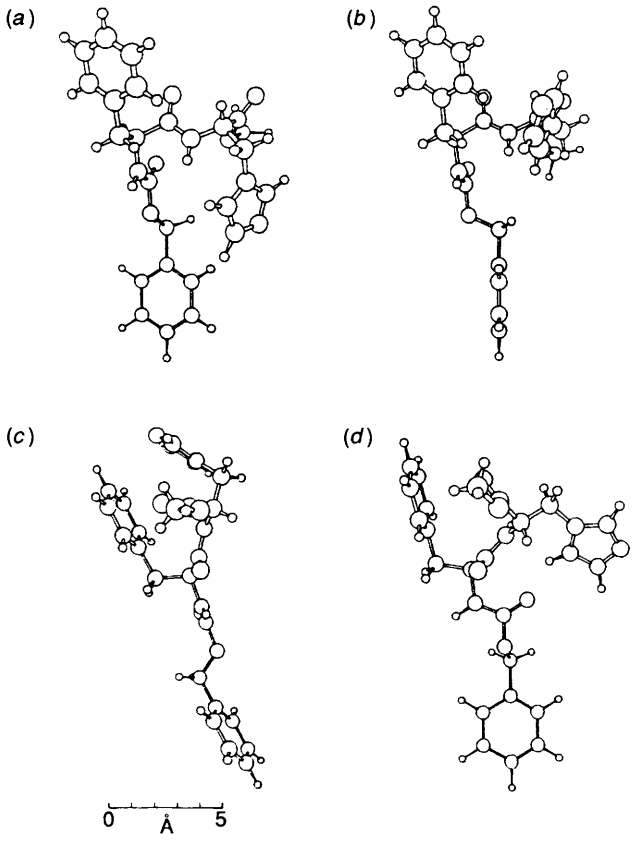

Fig. 5 Conformations of Z-Phe-His-OMe (7) with the lowest energies

conformers (Fig. 5) show full penetration of the side chain units of L-Phe and L-His around the benzyloxy sidearm axis. These conformers show only minor deviations from the planarity in the benzyloxy sidearm. In some of the catalyst conformations a histidyl group is well positioned for attack on the carbonyl group of the L enantiomer. Next, an attempt was made to find a stereochemical correlation between the catalyst and substrate. The conformer **7a** was selected in this study because a similar structure was derived from the inspection of hand-held CPK molecular models. The geometries of model **7a** and Ac-Phe-OMe, along with the atomic charges obtained from a MNDO semiempirical calculation, are shown in Fig. 6.

Fig. 7(*a*) shows CPK space filling models of conformer **7a** of ZPhe-His-OMe and Ac-Phe-OMe obtained from the computer calculation. The side chains of L-Phe and L-His in Z-Phe-His-OMe constitute a hydrophobic area through the intramolecular interactions between amino acid residues as well as hydrogen bonds between amide parts in the dipeptide catalyst. A fitting by CPK models of Ac-Phe-OMe and Z-Phe-His-OMe through the efficient hydrophobic and/or recognizant interactions between the substrate and the catalyst is presented in Fig. 7(*b*). On the other hand, it is suggested that the interaction between D-Phe in the substrate and L-Phe in the catalyst might bring an unfavourable fitting and a histidyl group is not positioned for attack on the carbonyl group in the course of the reaction. These computer-generated structures were consistent with the available experimental data, allowing the methodology to be extended to the interaction of the catalyst with the substrate in the presence of micelles.

Conclusions.—The present study clearly shows that some of the dipeptide derivatives (Z-Leu-His and Z-Phe-His) are effective stereoselective catalysts for cleavages of the enantiomeric substrates. The kinetic results indicate that the stereoselective control is mainly determined by catalytic acyl transfer to the

Fig. 7 CPK space filling model of (*a*) Ac-Phe-OMe and Z-Phe-His-OMe and (*b*) a fitting model of Ac-Phe-OMe and Z-Phe-His-OMe

(Facing p.546)

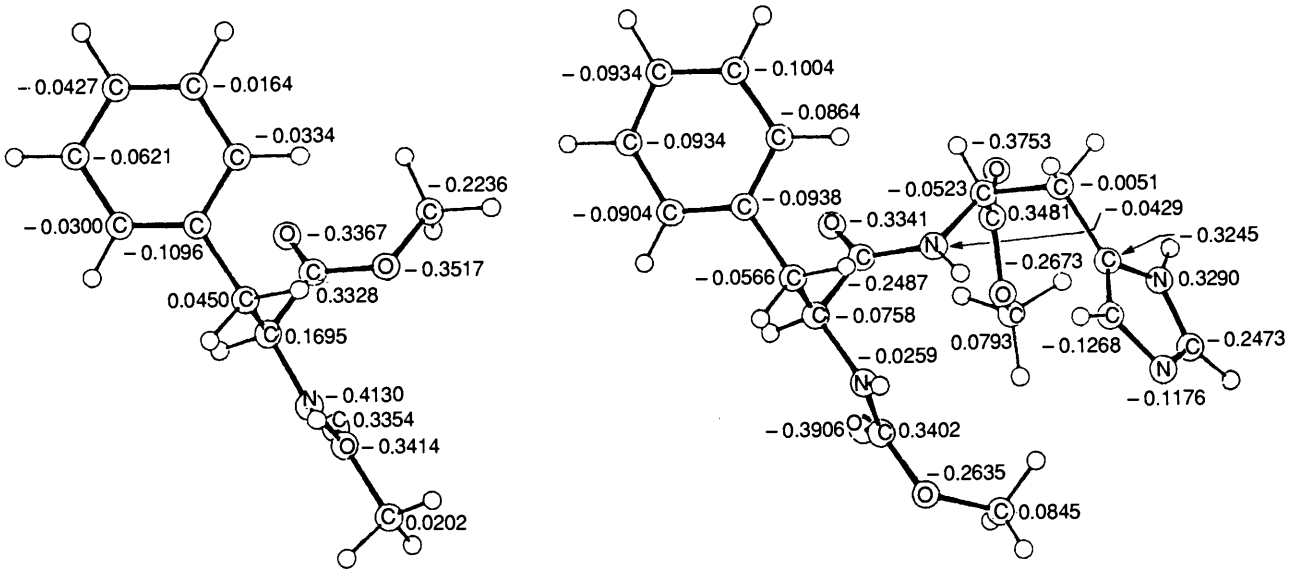

Fig. 6 Molecular structures of Ac-Phe-OMe and the model catalyst derived from semiempirical MNDO calculations. The numbers adjacent to each heteroatom are the atomic charges.

Table 4 Torsional angles of Z-Phe-His-OMe (7) with the minimum energies

		Torsional angles/°									
Conformer[a]	Energy	θ_1	φ_2	ψ_2	χ_2^1	χ_2^2	φ_3	ψ_3	χ_3^1	χ_3^2	θ_4
7a	−2.1	−123	−71	−42	178	71	−61	−40	64	87	179
7b	−1.7	−100	−66	−46	175	−105	−69	−39	−59	101	179
7c	−3.6	112	−156	144	−176	−107	−60	134	57	−95	−178
7d	−1.5	102	−71	140	177	79	−70	101	−60	−75	179
7e	−2.2	−108	−155	142	174	−106	−63	109	177	68	180
7f	−2.0	−42	−64	−44	175	77	−65	−41	58	−97	178

[a] Starting conformations; **7a–b**, α-helix; **7c–d**, β-sheet (parallel); **7e**, β-sheet (antiparallel); **7f**, turn (type I).

imidazole function at the active site of the optically-active catalyst. These catalysts might have the appropriate orientation of the functional group and a stereochemical fit with the combination of specific interactions such as steric, hydrophobic and hydrogen bonding. A model proposed for the evaluation of the interaction between Z-Phe-His-OMe and Ac-Phe-OMe has been studied by an empirical calculation method. The computational studies do find a stable structure for Z-Phe-His-OMe which is consistent with the model proposed in terms of intramolecular interactions between amino acid side residues as well as hydrogen bonds between amide parts. Indeed, experimental and computational findings for analogous systems support this idea. An analysis of conformers at their energy minima obtained from the calculation reproduces the sense of the kinetic stereoselectivities. The present results may suggest a rational approach to the design of highly stereoselective catalysts in surfactant aggregate systems.

Acknowledgements

We are grateful to Professor Atsushi Sugii of Kumamoto University for providing CD data. The authors also thank the Computer Centre of the Institute for Molecular Science, for the use of the Hitac M-680H computer and the Library Program MNDOC (IMS). This work was supported in part by a Grant-in-Aid for Scientific Research from the Ministry of Education, Science, and Culture, Japan.

References

1 M. L. Bender, *Mechanisms of Homogeneous Catalysis from Protons to Proteins*, Wiley-Interscience, New York, 1971.

2 (*a*) J. H. Fendler and E. J. Fendler, *Catalysis in Micellar and Macromolecular Systems*, Academic Press, New York, 1975; (*b*) C. A. Bunton, *Application of Biochemical Systems in Organic Chemistry*, part 2, eds. J. B. Jones, C. J. Sih and D. Perlman, Wiley, New York, 1975.

3 (*a*) C. A. Bunton, J. Robinson and M. F. Stam, *Tetrahedron Lett.*, 1971, 121; (*b*) J. M. Brown and C. A. Bunton, *J. Chem. Soc., Chem. Commun.*, 1974, 969; (*c*) J. M. Brown, R. L. Elliott, C. G. Riggs, G. Helmchen and G. Nill, *Angew. Chem., Int. Ed. Engl.*, 1981, **20**, 890.

4 (*a*) R. A. Moss and W. L. Sunshine, *J. Org. Chem.*, 1974, **39**, 1083; (*b*) R. A. Moss, T. J. Lukas and R. C. Nahas, *Tetrahedron Lett.*, 1977, 3851; (*c*) R. A. Moss, R. C. Nahas and T. Lukas, *Tetrahedron Lett.*, 1978, 508.

5 J. Koga, M. Shoshi and N. Kuroki, *Nippon Kagaku Kaishi*, 1978, 1179.

6 (*a*) K. Yamada, H. Shosenji and H. Ihara, *Chem. Lett.*, 1979, 491; (*b*) K. Yamada, H. Shosenji, H. Ihara and Y. Otubo, *Tetrahedron Lett.*, 1979, 2529; (*c*) H. Ihara, S. Ono, H. Shosenji and K. Yamada, *J. Org. Chem.*, 1980, **45**, 1623; (*d*) S. Ono, H. Shosenji and K. Yamada, *Tetrahedron Lett.*, 1981, 2391.

7 (*a*) K. Kon-no, M. Tosaka and A. Kitahara, *J. Colloid Interface Sci.*, 1981, **79**, 581; (*b*) 1982, **86**, 288.

8 (*a*) Y. Murakami, A. Nakano, A. Yoshimatsu and K. Fukuya, *J. Am. Chem. Soc.*, 1981, **103**, 728; (*b*) Y. Murakami, A. Nakano, H. Ikeda, I. Imori and K. Akiyoshi, *Bull. Chem. Soc. Jpn.*, 1985, **58**, 172.

9 (*a*) R. Ueoka, T. Terao and K. Ohkubo, *Nippon Kagaku Kaishi*, 1980, 462; (*b*) K. Ohkubo, K. Sugahara, K. Yoshinaga and R. Ueoka, *J. Chem. Soc., Chem. Commun.*, 1980, 393; (*c*) K. Ohkubo, K. Sugahara, H. Ohta, K. Tokuda and R. Ueoka, *Bull. Chem. Soc. Jpn.*, 1981, **54**, 576; (*d*) K. Ohkubo, N. Matsumoto and H. Ohta, *J. Chem. Soc., Chem. Commun.*, 1982, 738.

10 (*a*) R. Ueoka and Y. Murakami, *J. Chem. Soc., Perkin Trans. 2*, 1983, 219; (*b*) R. Ueoka, Y. Matsumoto, T. Nagamatsu and S. Hirohata, *Tetrahedron Lett.*, 1984, 1363; (*c*) R. Ueoka and Y. Matsumoto, *J. Org. Chem.*, 1984, **49**, 3774; (*d*) R. Ueoka, Y. Matsumoto and Y. Ihara, *Chem. Lett.*, 1984, 1809; (*e*) R. Ueoka, R. A. Moss, S. Swarup, Y. Matsumoto, G. Strauss and Y. Murakami, *J.*

Am. Chem. Soc., 1985, **107**, 2185; (*f*) R. Ueoka, Y. Matsumoto, N. Takemiya and Y. Ihara, *Chem. Pharm. Bull. Jpn.*, 1989, **37**, 2263.
11 (*a*) Y. Ihara, *J. Chem. Soc., Chem. Commun.*, 1978, 984; (*b*) Y. Ihara, *J. Chem. Soc., Perkin Trans. 2*, 1980, 1483; (*c*) Y. Ihara, M. Nango and N. Kuroki, *J. Org. Chem.*, 1980, **45**, 5009.
12 (*a*) Y. Ihara, R. Hosako, M. Nango and N. Kuroki, *J. Chem. Soc., Chem. Commun.*, 1981, 393; (*b*) Y. Ihara, R. Hosako, M. Nango and N. Kuroki, *J. Chem. Soc., Perkin Trans. 2*, 1983, 5; (*c*) Y. Ihara, N. Kunimasa, T. Kunikiyo, M. Nango and N. Kuroki, *Chem. Lett.*, 1981, 667.
13 (*a*) Y. Ihara, Y. Kimura, M. Nango and N. Kuroki, *Makromol. Chem., Rapid Commun.*, 1982, **3**, 521; (*b*) Y. Ihara, Y. Kawamura, E. Nakanishi, M. Nango and J. Koga, *Macromol. Chem., Rapid. Commun.*, 1985, **6**, 829.
14 (*a*) Y. Ihara, N. Kunikiyo, T. Kunimasa, Y. Kimura, M. Nango and N. Kuroki, *J. Chem. Soc., Perkin Trans. 2*, 1983, 1741; (*b*) Y. Ihara, M. Okamoto, Y. Kawamura, E. Nakanishi, M. Nango and J. Koga, *J. Chem. Soc., Perkin Trans. 2*, 1987, 607; (*c*) Y. Ihara, E. Nakanishi, A. Akiyama and H. Yamamoto, *J. Polym. Sci., Polym. Chem. Ed.*, 1989, **27**, 87; (*d*) Y. Ihara, K. Igata, Y. Okubo and M. Nango, *J. Chem. Soc., Chem. Commun.*, 1989, 1900.
15 M. Nango, Y. Kimura, Y. Ihara and N. Kuroki, *Macromolecules*, 1988, **21**, 2330.
16 (*a*) R. Ueoka, Y. Matsumoto, T. Yoshino, T. Hirose, J. Kikuchi and Y. Murakami, *Chem. Lett.*, 1986, 127; (*b*) R. Ueoka, Y. Matsumoto, T. Yoshino, N. Watanabe, K. Omura and Y. Murakami, *Chem. Lett.*, 1986, 1743; (*c*) R. Ueoka, Y. Matsumoto, R. A. Moss, S. Swarup, A. Sugii, K. Harada, J. Kikuchi and Y. Murakami, *J. Am. Chem. Soc.*, 1988, **110**, 1588.
17 (*a*) F. A. Momany, R. F. McGuire, A. W. Burgess and H. A. Scheraga, *J. Phys. Chem.*, 1975, **79**, 2361; (*b*) M. Sisido, personal communication.
18 Y. Beppu, *Comput. Chem.*, 1989, **13**, 101.
19 (*a*) M. J. S. Dewar and W. Thiel, *J. Am. Chem. Soc.*, 1977, **99**, 4899; (*b*) W. Thiel, *J. Am. Chem. Soc.*, 1981, **103**, 1413, 1420.
20 I. Cho and G. Kim, *J. Org. Chem.*, 1988, **53**, 5189.
21 K. Ohkubo, M. Kawata, T. Oritto and H. Ishida, *J. Chem. Soc., Perkin Trans 1*, 1989, 666.
22 N. Harada and K. Nakanishi, *Circular Dichroic Spectroscopy Excition Coupling in Organic and Bioorganic Chemistry*, University Science Books, Mill Valley, CA, USA, 1983.
23 (*a*) G. Halzwarth and P. Doty, *J. Am. Chem. Soc.*, 1965, **87**, 218; (*b*) Y.-H. Chen, J. T. Yang and K. H. Chan, *Biochemistry*, 1974, **13**, 3350; (*c*) T. Higashijima, K. Wakamatsu, M. Takimitsu, M. Fujino, T. Nakajima, T. Miyazawa, *FEBS Lett.*, 1983, **152**, 227.
24 (*a*) IUPAC-IUB, *Biochemistry*, 1970, **9**, 3471; (*b*) P. N. Lewis, F. A. Momany, H. A. Scheraga, *Biochim. Biophys. Acta*, 1973, **303**, 211; (*c*) S. Miyamoto and M. Yoshimoto, *Chem. Pharm. Bull.*, 1985, **33**, 4856.

Paper 0/03355C
Received 24*th July* 1990
Accepted 25*th October* 1990